Hindawi
Advances in Materials Science and Engineering
Volume 2022, Article ID 9101820, 14 pages
https://doi.org/10.1155/2022/9101820

Research Article

Influence of End Milling Process Variables on Material Removal Rate and Surface Roughness of Direct Metal Laser Sintered Inconel 718 Plate

N. L. Parthasarathi,[1] Dhinakaran Veeman,[2] Duraisami Dhamodharan,[3,4] Utpal Borah,[1] M. Ravichandran,[5] L. Natrayan,[6] and Wubishet Degife Mammo[7]

[1]*Indira Gandhi Centre for Atomic Research, Kalpakkam 603102, India*
[2]*Centre for Additive Manufacturing, Chennai Institute of Technology, Chennai 600069, Tamil Nadu, India*
[3]*Department of Chemical and Biomolecular Engineering, Chonnam National University, Yeosu, Jeonnam 59626, Republic of Korea*
[4]*Greenlab, Department of Prosthodontics, Saveetha Dental College and Hospitals, Saveetha Institute of Medical and Technical Sciences, Chennai 600077, India*
[5]*K. Ramakrishnan College of Engineering, Samayapuram, Trichy 621112, India*
[6]*Department of Mechanical Engineering, Saveetha School of Engineering SIMATS, Tamil Nadu, Chennai 602105, India*
[7]*Mechanical Engineering Department, Wollo University, Kombolcha Institute of Technology, Kombolcha, South Wollo 208, Amhara, Ethiopia*

Correspondence should be addressed to Dhinakaran Veeman; dhinakaranv@citchennai.net and Wubishet Degife Mammo; wubishetdegife7@gmail.com

Received 11 November 2021; Revised 15 August 2022; Accepted 25 August 2022; Published 25 September 2022

Academic Editor: Fuat Kara

This study intends to optimize the end milling process variables for additively manufactured (AM) Inconel 718 alloy through the direct metal laser sintered (DMLS) method. Surface roughness and material removal rate have been considered as output responses. The end milling experiments were conducted using the design of experiments with an L_9 orthogonal array (OA) by varying the process variables like feed rate (mm/min), cutting speed (m/min), and depth of cut (mm). Taguchi technique was used to optimize the process variables. Examination of the variance table is working to regulate each variable's percentage contribution and significance in end milling experiments. The chip morphology of the DMLS Inconel 718 plate reveals that, at lower cutting speed, irregular and discontinuous chips were formed.

1. Introduction

In recent years, additive manufacturing (AM) technologies have more prominent features due to their advantages: cost-effectiveness, reduced lead time and waste, multiscale structure design, and design freedom [1, 2]. Highly complex and tailored products using materials such as metals, polymers, and ceramics in various forms such as powder, sheet, and filaments were produced using additive manufacturing technologies [3, 4]. Due to various environmental concerns, the conventional manufacturing process consumes more material and energy. So, the industries are now concentrating on imposing additive manufacturing technologies to develop metallic components [5, 6]. Compared with the conventional manufacturing process of superalloys, the additive manufacturing process has several advantages of flexibility and designability over the traditional process. Helical drilling was adopted instead of traditional drilling to make holes in superalloys, reducing the axial cutting force by ten times and improving the surface morphology of the machined surfaces [7]. Similarly, this AM technique cut down secondary costs like material and machining costs and vice versa [8, 9].

There are numerous metal additive manufacturing processes, but the direct metal laser sintering process possesses several advantages, such as localised high heat input within a short time interval. The production of superalloys using the DMLS method warrants defect-free surfaces [10]. Dinda et al. have prepared Inconel 625 alloy by using the DMLS method; the prepared alloys are defect-free (crack and porosity) [11]. Nickel-based superalloys have huge market potential and are more suitable for applications such as nuclear, medical, aerospace, and chemical industries. Inconel 718 alloy has excellent creep, fatigue, and corrosion resistance. Due to its excellent stability and strength at a high temperature of around 700°C, Inconel 718 was deployed [12]. Inconel 718 has been used to manufacture hot sections in the aerospace components such as turbines and engines [13]. During machining, Inconel 718 alloy has poor thermal conductivity and high chemical affinity, which results in hard machining or cutting the material [14]. In this milling operation, the tool and the workpiece are in contact. There is a generation of higher importance of stress at the contact point, which results in a massive volume of heat and a steep rise in temperature at the cutting zone. This leads to a chance of adhesion of the worn particles in the cutting tool, resulting in more chances of tool wear. It also impacts the tool's life and the cutting process's quality [15]. So, a process optimization study is needed for the respective machining conditions of the additively manufactured Inconel 718 superalloy.

In the milling of superalloys like Inconel 718, the surface quality of the machined surface is to be measured by using the material removal rate and surface roughness. Surface quality is affected by the type of materials and workpiece involved in the machining. Apart from that, the machining conditions like cutting parameters, tool wearing, machine vibration, and other external factors influence the surface roughness of the machined surfaces. So as to improve the surface finish of the materials, it is undergone for milling operation, and there is a need for optimizing the process conditions and variables of the end milling operation.

Researchers worldwide have endeavoured to study the surface characteristics and optimization of the milling process variables of newly engineered materials. Thepsonthi and Ozal studied particle swarm optimization to minimalize the surface roughness of the milling operation of titanium alloy. The results show that the feed rate has tremendously affected the optimization of surface roughness of the machined surfaces [16]. Likewise, Ma et al. studied the high-speed milling process on Inconel 718 alloy and optimized the process variables such as surface roughness and machining time using grey relational analysis [17]. The results show that increases in the feed rate have a major effect on the frictional force. Anburaj and Pradeepkumar have studied the process optimization of face milling on Inconel 625 superalloy using TOPSIS analysis. The results highlight that the highest closeness coefficient was observed for the conditions such as a cutting speed of 80 m/min and a feed rate of 0.05 mm/tooth in a cryogenic environment [18]. Jiang et al. investigated the effect of cutting process variables on average surface roughness (Ra) under various cooling/lubrication conditions, with minimal quantity lubrication and dry and wet cutting in Ti6Al4V alloy. The quadratic equation reported the optimal average surface roughness values [19]. Sarkar et al. studied the impact of machining parameters concerning the end milling process and the response variables, such as surface finish to be measured in the Inconel 718 material. The results show that the cut's depth significantly influences the surface roughness measurement for the milling operation [20]. Shihab et al. studied the optimization of the end milling process on the aluminum 7075 metal matrix composites. The experiment was conducted by varying the process variables such as feed rate, spindle speed, depth of cut, and volume of the reinforcement percentage. The study shows that the lowest surface roughness value of 1.29 μm was observed on the optimal experimental parameter combinations [21]. Even though several studies have been conducted in superalloys, titanium alloys, and aluminum alloys correlating machining parameters with surface roughness values, the current study involving analysing the surface roughness values of Inconel 718 in end milling and correlating it with milling parameters seeks to shed light on the finishing process of additive manufactured components. The study's outcome is required to enhance the milling process conditions of the prepared DMLS Inconel 718 plate, and this idea will give first-hand knowledge to the industry.

The present work encompasses the process enhancement of the end milling process for the DMLS Inconel 718 plate. The impact of feed rate, depth of cut, and spindle speed was optimized (using the Taguchi technique with MINITAB 20 software) for surface roughness and material removal rate. Chip morphology of the machined DMLS plate was characterized using scanning electron microscopy (SEM).

2. Materials and Methods

2.1. Preparation of DMLS Inconel 718 Plate. In this study, Inconel 718 superalloy was produced using DMLS. Initially, Inconel 718 alloy powder was chosen as a candidate material for component fabrication. Figure 1(a) shows the build orientation of the Inconel part to be fabricated. The Inconel 718 samples are produced on the substrate by directly melting the Inconel 718 powders using the M 280 Direct Metal Laser Sintering RP machine. The Inconel plate fabrication machine is shown in Figure 1(b). The quality of the plate is based on the size of the particle used for the fabrication of the component. As per the ASTM standards, the particles were sieved mechanically, and flow analysis and particle size analysis were done before part fabrication.

The plates are built with respective dimensions, and the design was incorporated into the CATIA CAD model. The prepared CATIA CAD model was saved in STL format for properly slicing the component into thin cross-sections and for building the parts free from errors with good accuracy of the components.

A dimension of $40 \times 40 \times 10$ mm cross-section sample was built on the 25 mm thick EN 24 substrates. A high-powered laser source (Ytterbium fibre laser) of 2000 W is supplied to melt the metal powders and build the components on the metal substrates. Build parts are enclosed in the inert atmosphere (argon). Table 1 shows the build parameters and selection to build the Inconel 718 alloy. Fine-tuned

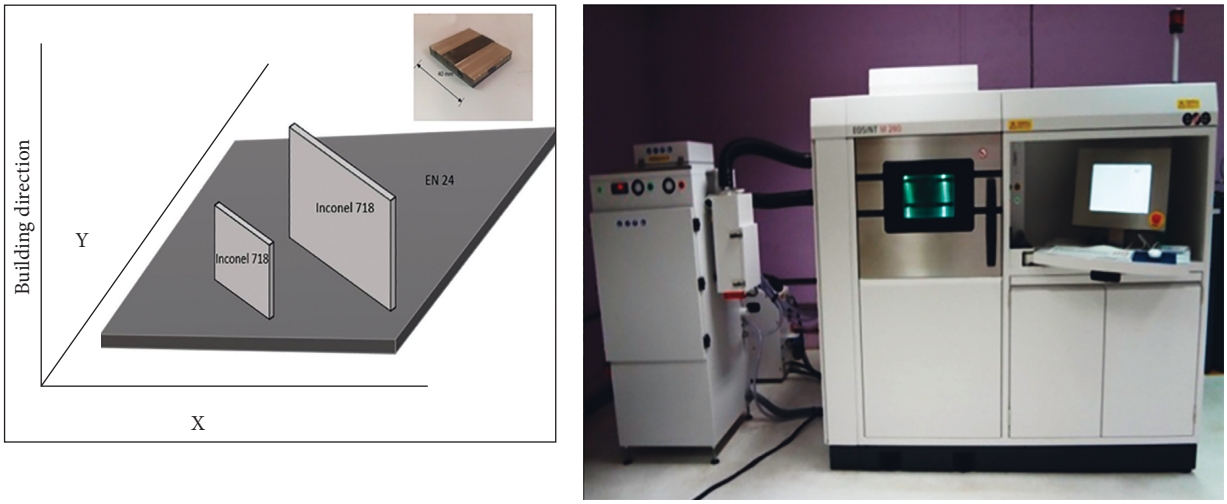

(a) (b)

Figure 1: (a) Build orientation of DMLS component with sample for milling experiment and (b) M 280 Direct Metal Laser Sintering RP machine.

Table 1: Parameters for fabricating Inconel 718 plate.

Parameter	Value
Layer thickness	100 microns
Scan speed	7.0 m/s
Powder particles	20 microns
Build direction	Vertical
Laser power	2000 W
Platform preheat	80°C
Part orientation	15°C inclined vertical
Recoating speed	100 mm/s

laser and Inconel powders are used from the overall optimized parameters for the part preparation. The prepared plate looks like forged parts in density, and its strength is free from porosity. The produced parts are 99% dense and free from porosity. Postprocessing processes like heat treatment greatly surpass the porosity of the produced Inconel 718 parts. The nominal composition of the Inconel 718 alloy and EN8 steel was measured using X-ray fluorescence (XRF) analysis, tabulated in Table 2.

The prepared additive manufactured components undergo a postprocessing process to improve their surface roughness and remove external supports and internal stress in the build parts. Additively manufactured components exhibit a high surface roughness value of 6–8 μm, which is unsuitable for various applications. To reduce the prepared additively manufactured Inconel 718 alloy's surface roughness, finishing processes such as milling, deburring, buffing, and polishing are required to attain less than 2 μm [22].

2.2. Experimental Procedure. DMLS Inconel 718 plate was selected as the sample for investigating the effect of various milling process variables. The sample for milling is shown in Figure 2(a). The end milling process was done in a CNC vertical machining centre (DT110, Mikrotools) and is shown in Figure 2(b). The coolant was supplied in the cutting zone with the help of a setup MiQuel BASE, DROPSA. GMG27080 type end mill cutter is used for the end milling operation and has a 5-flute variable helix angle. The specifications of the milling cutter will be a shank diameter of 8 mm, diameter tolerance is h6, and the detailed tool specification is shown in Figure 3. A water-miscible coolant named Blastocut 4000 is deployed during the machining. It comprises 10~12% coolant mixed with water to ensure that the coolant is sufficiently greasy to reduce the heat generated during the cutting operation. The deployment of coolant was intended at the tooltip, enabling the exposure with the workpiece and thereby addressing the chip's origination.

2.3. Optimization of End Milling Variables. For designing the end milling experiments, three factors, namely, spindle speed, feed rate, and depth of cut [20], were considered three levels of each factor. The experimental design and parameters for the end milling process are shown in Table 3. Using the experiments' design, the L9 orthogonal array was designed for end milling processes by using the experiments' design. The set of 9 different experimental conditions is planned by varying the parameters and levels of each set of conditions shown in Table 4. Material removal rate and arithmetic (Ra) surface roughness are the output responses for the optimization process. Taguchi and examination of variance techniques are carried out to decide the optimal combination for obtaining the least surface roughness of the machined surface and maximum material removal rate [23].

During the milling operation, the weight of the sample was measured before and after every step of the milling experiments. Likewise, the running time for the tests was noted for computing the material removal rate. The material removal rate is computed using the measured data, such as changes in the material weight and time taken for the machining.

Table 2: Nominal composition of Inconel 718.

Elements (wt%)	Ni	Cr	Nb	Mo	Ti	Al	Co	Cu	C	Fe
As received	50	21	4.97	2.8	0.65	0.2	1	0.3	0.08	Bal.
DMLS IN718	51.48	19.58	5.15	3.89	0.97	0.87	0.37	0.18	0.015	Bal.

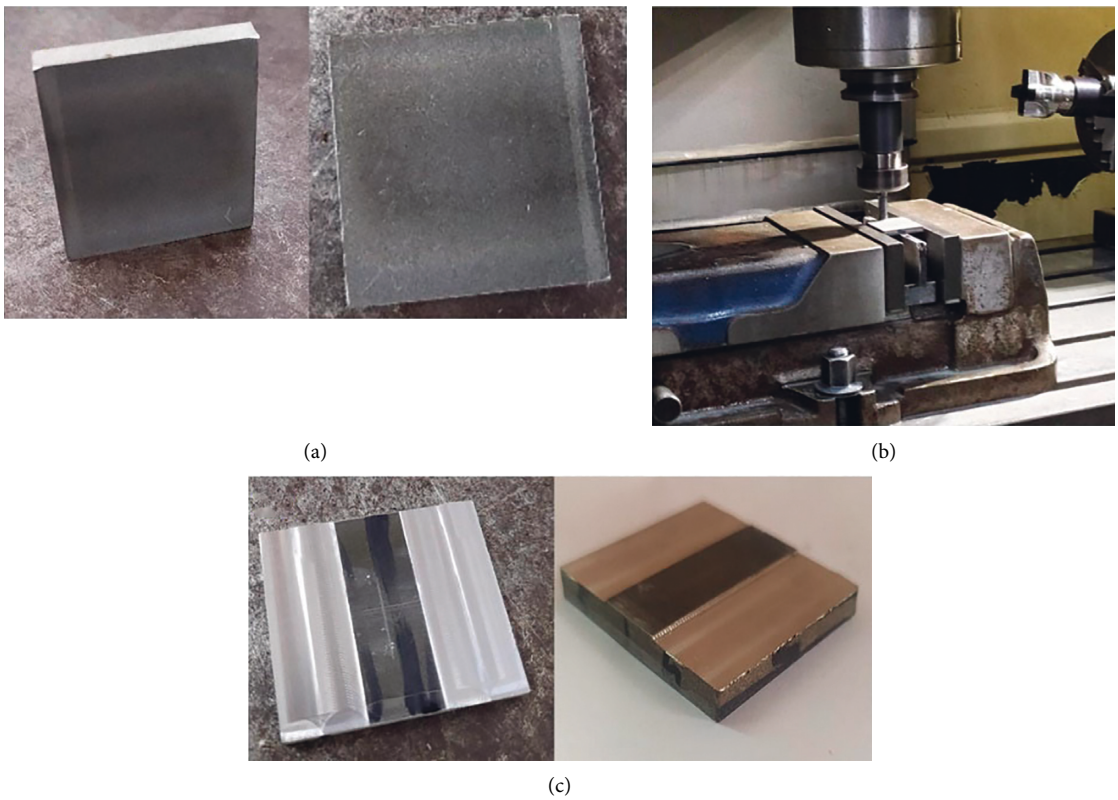

(a) (b) (c)

Figure 2: (a) DMLS Inconel 718 sample, (b) milling process, and (c) machined sample.

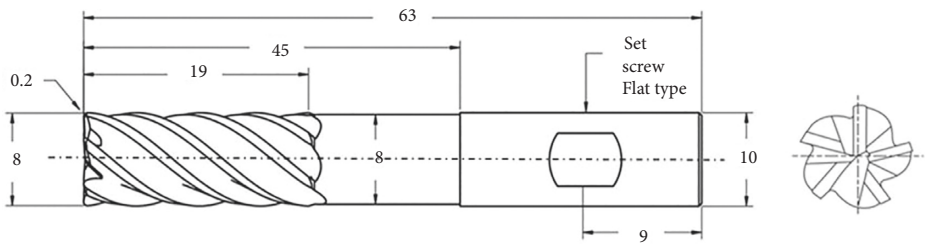

All dimensions are in "mm."

Figure 3: Cutting tool dimensions.

Table 3: Process variables (factors/levels).

Parameters	Level		
	1	2	3
Cutting speed (m/min)	75	100	125
Feed rate (mm/min)	50	75	100
Depth of cut (mm)	0.1	0.2	0.3

$$\text{MaterialRemovalRate} = \frac{\left(W_f - W_i\right)}{\left(\rho_i * t\right)}. \quad (1)$$

W_f and W_i represent the sample weight before and after machining, ρ_i represents the density of the prepared DMLS plate, and t represents the time taken for the milling operation. Similarly, the other output response, such as surface roughness of each machined condition, was noted using a 3-dimensional surface profilometer (TALYSURF CLI 1000 surface profilometer). The maximum material removal rate

Table 4: Orthogonal array (L_9) and its output responses for the end milling experiments.

Experiment no.	Cutting speed (m/min)	Feed rate (mm/min)	Depth of cut (mm)	MRR (mm^3/min)	Surface roughness (μm)	SNRA-1	MEAN-1	SNRA-2	MEAN-2
1	75	50	0.1	630	0.69	55.98681	630	3.223018	0.69
2	75	75	0.2	1052	0.74	60.44031	1052	2.615366	0.74
3	75	100	0.3	1580	0.82	63.97314	1580	1.723723	0.82
4	100	50	0.2	789	0.61	57.94154	789	4.293403	0.61
5	100	75	0.3	1256	0.7	61.97979	1256	3.098039	0.7
6	100	100	0.1	994	0.648	59.94773	994	3.7685	0.648
7	125	50	0.3	1098	0.545	60.81205	1098	5.27207	0.545
8	125	75	0.1	974	0.635	59.77118	974	3.944525	0.635
9	125	100	0.2	1491	0.775	63.46955	1491	2.213966	0.775

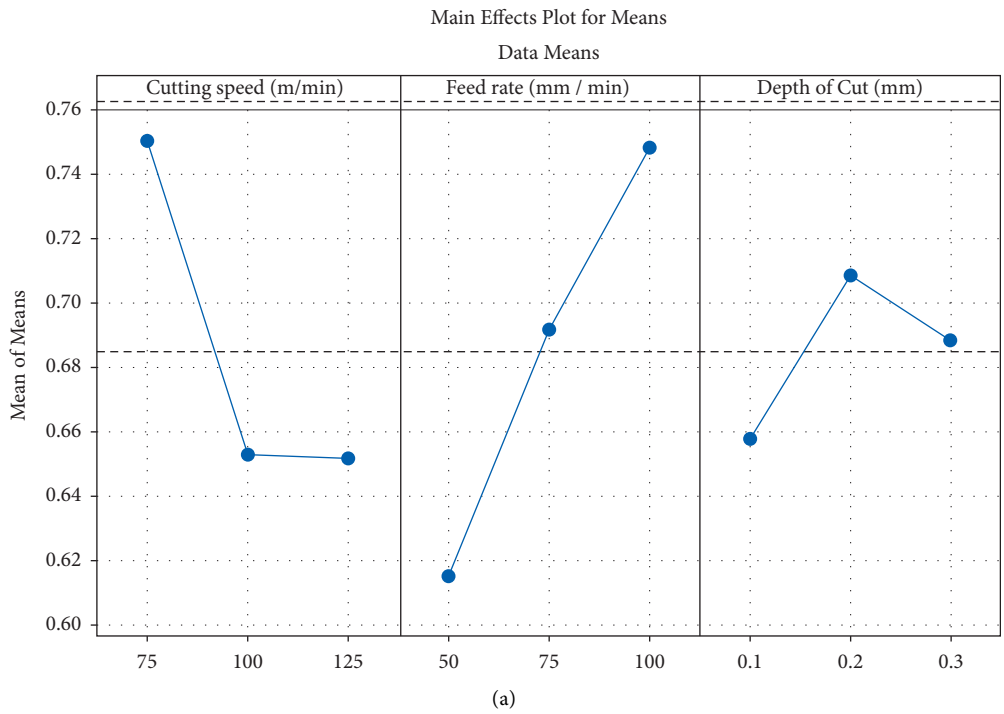

(a)

Figure 4: Continued.

(b)

Figure 4: (a) Means plot for the surface roughness of milled AM component. (b) S/N ratio plot for the surface roughness of milled AM component.

and lowest surface roughness are taken as the output response parameter for enhancing the end milling analysis of DMLS Inconel 718 alloy. The experimental results are converted as an S/N ratio for the output responses of the end milling process. The quality characteristics of the S/N ratio studied for optimization in Taguchi analyses are smaller-the-best, nominal-the-best, and larger-the-best. In this study, larger-the-best was considered for material removal rate and smaller the best was considered for surface roughness. The expression for the respective response is shown in the following equation:

$$S/N = -10 * \log_{10}\left(\frac{1}{Y^2}\right). \quad (2)$$

Y denotes the response, such as the material removal rate of the end milling process experiments.

$$S/N = -10 * \log 10\left(\text{sum}\frac{Y^2}{N}\right). \quad (3)$$

Y denotes the response, such as the surface roughness of the end milling process experiments.

The statistical study was led by the MINITAB 20 statistical software tool. Scrutiny of alteration technique is followed to discover the most influencing factor regarding the various experimental conditions. In the present milling study, the 95% confidence limit and 5% importance level were set to catch on the interaction of each parameter. From the experimental results, the most influencing factors were selected. The input parameters include cutting speed, depth of cut, and feed rate. Furthermore, the regression equation and model for the best fit were predicted with independent factors (cutting speed, depth of cut, and feed rate) and dependent on surface roughness and material removal rate.

2.4. Characterization of Machined DMLS Plate Surface and Its Chips. The TALYSURF CLI 1000 surface profilometer measured the arithmetic average deviation of the roughness profile (Ra) values. The milled surfaces are also further analysed to measure the arithmetic mean deviation of the surface (Sa) by the same measuring instruments. The chip morphology of the machined AM Inconel 718 alloy was observed in the scanning electron microscopy (JEOL Ltd., JCM-6000 Versatile Benchtop SEM) to define the chip breakdown pattern during the end milling operation.

3. Results and Discussion

Initial analytical conditions and preliminary trials are done before starting the experiment with the L-9 orthogonal array. After the milling experiment on the DMLS Inconel 718 plate, the experimental output like surface roughness and material removal rate was measured. The optimal cutting conditions were discussed in the following sections.

3.1. Parametric Optimization of Surface Roughness Analysis for the AM Component. Figures 4(a) and 4(b) demonstrate the main plot for the S/N ratio values of the surface roughness variable for each constraint: feed rate, cutting speed, and depth of cut. This study reported that each parameter effect relates to the milling characteristics of the DMLS Inconel 718 plate. From the overall observed results,

the feed rate and cutting speed impact the milling study about the surface roughness response on the DMLS Inconel 718 plate. The cutting speed directly correlates with the surface roughness of the machined DMLS Inconel 718. Figure 4(a) gives the end milling experiment's factor (cutting speed). The experiment was demonstrated with variable factors like 75, 100, and 125 m/min. The lowest surface roughness value of 0.6517 μm was observed at the highest cutting speed.

For DMLS Inconel 718 alloy, at a higher cutting speed, there is a chance of generation of higher temperature at the contact zone; this is due to the poor thermal conductivity of Inconel alloy. In case of a higher cutting speed, it produces a smooth surface finish compared to the lower cutting speed. It is because there is a chance of generating higher heat at the shear cutting zone at a higher cutting speed. It causes a smooth surface concerning the workpiece material softening. Kayanka et al. also reported a similar observation on the milling of superalloy [24]. Figure 4(b) shows the factor (feed rate) with variable levels of 50, 75, and 100 mm/min. The highest signal-to-noise ratio of 0.7477 μm was observed on the higher feed rate at 100 mm/min. As the feed rate rises, there is a rise in the S/N ratio value for the respective surface roughness. An increase in the feed rate shows an increase in the surface roughness of the machined surfaces. The increase in the surface roughness at a higher feed rate condition is a chance of increasing the chip thickness, resulting in the generation of higher force and heat at the contact point. This may lead to the chatter of the cutting tool and a higher chance of tool wear resulting in a poor surface finish at a higher feed rate. Similar outcomes were also obtained by Zahoor et al. on the AISI P20 tool steel in the vertical milling operation [25]. Nevertheless, the depth of cut does not significantly impact the milling operation concerning the surface roughness parameter.

The results show that increases in the depth of cut show increases in the surface roughness of the machined surface. It is due to the higher depth of cut; a large volume of heat input is generated, resulting in increases in the surface roughness. From the overall milling experimental results regarding the surface roughness responses, the optimal combination for the lowest surface roughness value will be the lowest feed rate of 50 mm/min, the highest cutting speed of 125 m/min, and the lowest depth of cut of 0.1 mm. The delta value was calculated to measure the most influential factor for the end milling experiment. Table 5 shows the measured responses of surface roughness for the machined surfaces. The delta value was calculated based on the difference in the maximum and minimum value of the signal-to-noise factor of the respective control factors. The influencing variable sequences are ordered from the milling experimental results of the DMLS Inconel 718 plate. Feed rate > cutting speed > depth of cut is the most significant variable, and the feed rate has a higher delta value of 0.1327, as shown in Table 5.

3.2. Parametric Optimization of Material Removal Rate Analysis for the DMLS Plate. Figures 5(a) and 5(b) indicate the S/N ratio plot for the material removal rate regarding process parameters like cutting speed, feed rate, and depth of cut. The maximum signal-to-noise ratio of 1355, 1311, and 1187 was observed on the higher feed rate of 100 mm/min, depth of cut of 0.3 mm, and higher cutting speed of 95 m/min. In all the cases, higher feed, depth of cut, and cutting speed exhibit high material removal rate. So this indicates that the material removal rate is directly proportional to the cutting parameters of the end milling operation. From the experimental results, with increases in the feed rate and depth of cut, there is a higher chance of producing a higher chip thickness of the machined DMLS Inconel 718 alloy. It is due to the higher feed rate and depth of cut. The cutting tool's indentation depth increases, resulting in a high material removal rate. Lu et al. also observed a similar outcome trend in the micromilling of Inconel 718 alloy. The result shows that the feed rate significantly influences the material removal rate [26].

The optimal combination for obtaining high material removal rate of DMLS Inconel 718 alloy will be a cutting speed of 125 m/min, feed rate of 100 mm/min, and depth of cut of 0.3 mm. Based upon the higher delta value, the most influential variable for milling DMLS Inconel alloy will be decided. The response table for each cutting condition and delta value is indicated in Tables6 and 7, which show the mean value for each cutting condition of Inconel 718 alloy. From the studied results, the higher delta value of 516 was obtained for the process parameter feed rate, followed by the depth of cut with a delta value of 445.3 and cutting speed with a delta value of 174. And the sequence of influencing variables concerning the rank is feed rate > depth of cut > cutting speed, which is also shown from the surface roughness graph at three different levels of depth of cut shown in Figures 6(a)–6(f). From the inclusive results, the material removal rate's major influencing variable is feed rate and depth of cut.

3.3. Analysis of Variance (ANOVA) Table. The statistically significant factors affecting the output responses, such as material removal rate and surface roughness of the end milling process for the AM Inconel 718 alloy, have been analysed using ANOVA analysis. The ANOVA analysis evaluated the percentage contributions of each factor regarding the surface roughness and material removal rate. ANOVA results for the surface roughness and material removal rate are carried out with a 95% confidence limit and a 5% significant level. It was maintained constant throughout the experiment [27] and is tabulated in Table 8.

For the milling experiment of DMLS Inconel 718 alloy, the feed rate, depth of cut, and cutting speed have influenced the material removal rate by 52.94%, 39.56%, and 6.11%, and the parameters which are significant with the response material removal rate and the P values are in the acceptable range lower than 0.05. So the results are significantly valid. Similarly, the most influential parameter concerning surface roughness in the end milling operation of DMLS Inconel 718 alloy will be a feed rate of 45.34%, followed by a cutting speed of 32.61% and a depth of cut of 6.66%. Apart from that, the depth of cut has a minimal contribution to the surface roughness for the end

Table 5: Response mean table for SNR on surface roughness of the machined DMLS Inconel 718 alloy response table for means.

Level	Cutting speed (m/min)	Feed rate (mm/min)	Depth of cut (mm)
1	0.7500	0.6150	0.6577
2	0.6527	0.6917	0.7083
3	0.6517	0.7477	0.6883
Delta	0.0983	0.1327	0.0507
Rank	2	1	3
Response table for signal-to-noise ratios (smaller is better)			
Level	Cutting speed (m/min)	Feed rate (mm/min)	Depth of cut (mm)
1	2.521	4.263	3.645
2	3.720	3.219	3.041
3	3.810	2.569	3.365
Delta	1.289	1.694	0.604
Rank	2	1	3

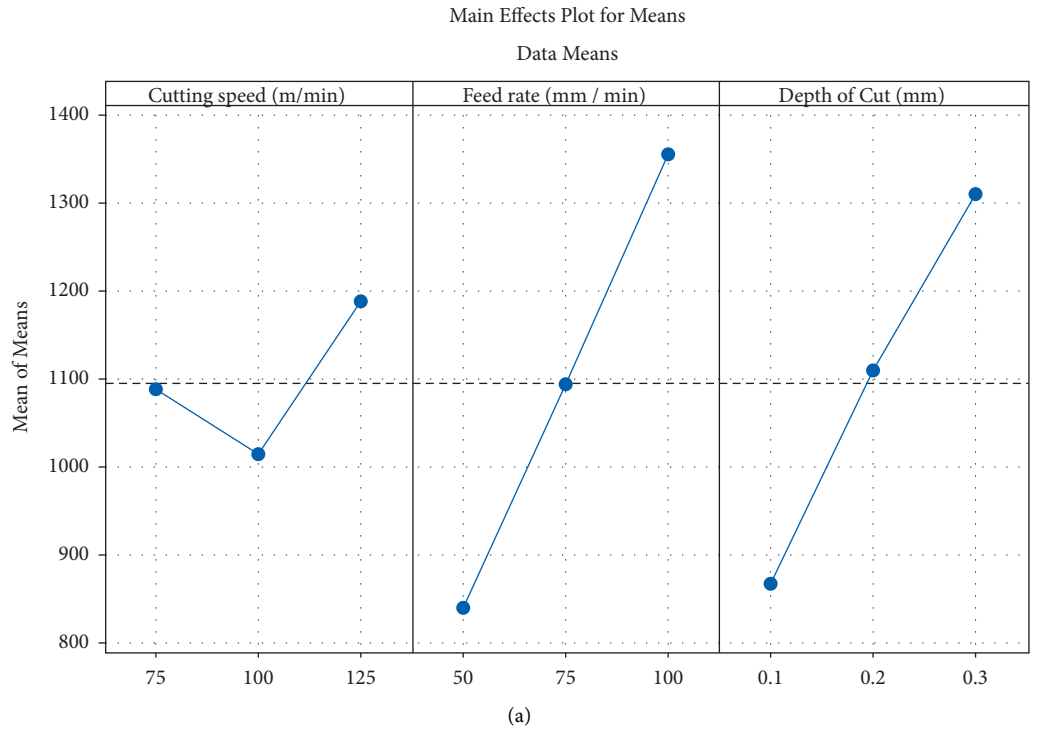

(a)

Figure 5: Continued.

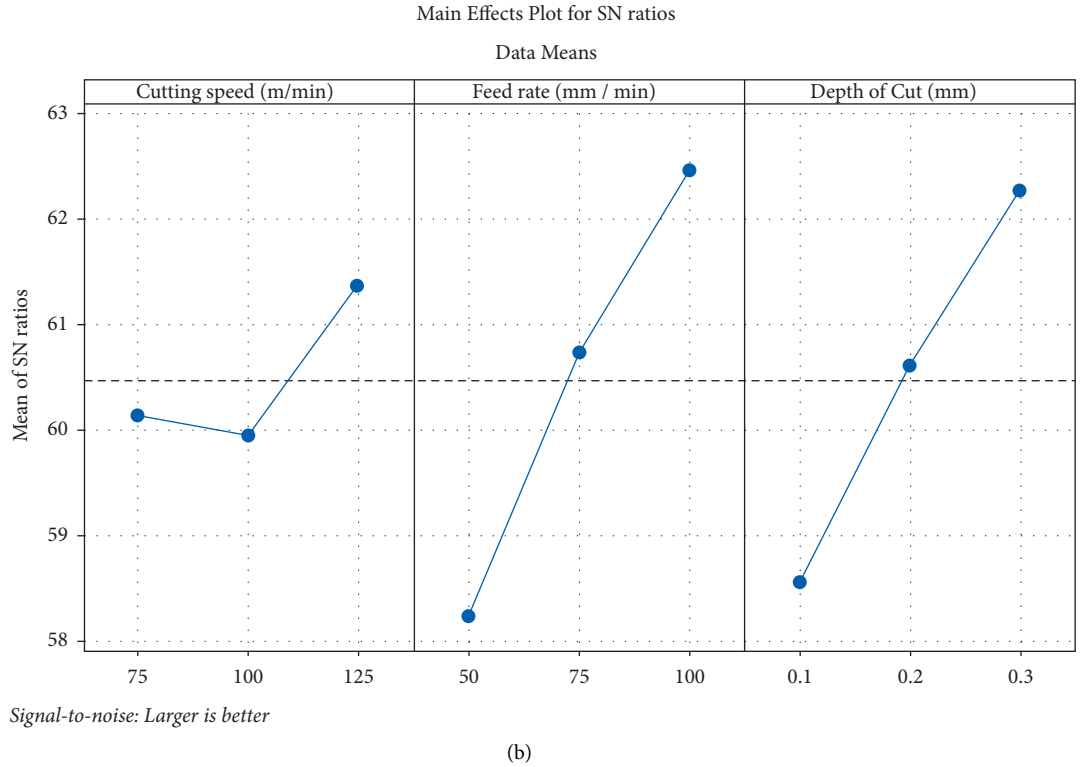

(b)

Figure 5: (a) Means of S/N ratio plot for the material removal rate of milled DMLS plate. (b) S/N ratio plot for the material removal rate of milled DMLS plate.

Table 6: Response table for means for each cutting condition of Inconel 718 alloy.

Level	Cutting speed (m/min)	Feed rate (mm/min)	Depth of cut (mm)
1	60.13	58.25	58.57
2	59.96	60.73	60.62
3	61.35	62.46	62.25
Delta	1.39	4.22	3.69
Rank	3	1	2

Table 7: Response table for S/N ratio for each cutting condition of Inconel 718 alloy.

Level	Cutting speed (m/min)	Feed rate (mm/min)	Depth of cut (mm)
1	1087.3	839.0	866.0
2	1013.0	1094.0	1110.7
3	1187.7	1355.0	1311.3
Delta	174.7	516.0	445.3
Rank	3	1	2

milling study of DMLS Inconel 718 alloy. The percentage contribution for the surface roughness and material removal rate based on the ANOVA analysis is shown in Figure 7.

3.4. Regression Analysis. The analytical outcomes established the regression equation by changing the input parameters, such as cutting speed, feed rate, and depth of cut, concerning the output responses, such as material removal rate and surface roughness. With the aid of MINITAB statistical software [28], the mathematical models were advanced for output retorts like surface roughness and material removal rate in DMLS Inconel 718 alloy milling. Using the regression equation, the *R*-square value was plotted against the predicted value and the retort parameters experimental value, such as material removal rate and surface roughness. Figure 8 shows the *R*-square value of the material removal rate and surface roughness relating to the DMLS 718 Inconel alloy milling process.

The experimental results clearly show that the *R*-square value based on the output response, such as material removal

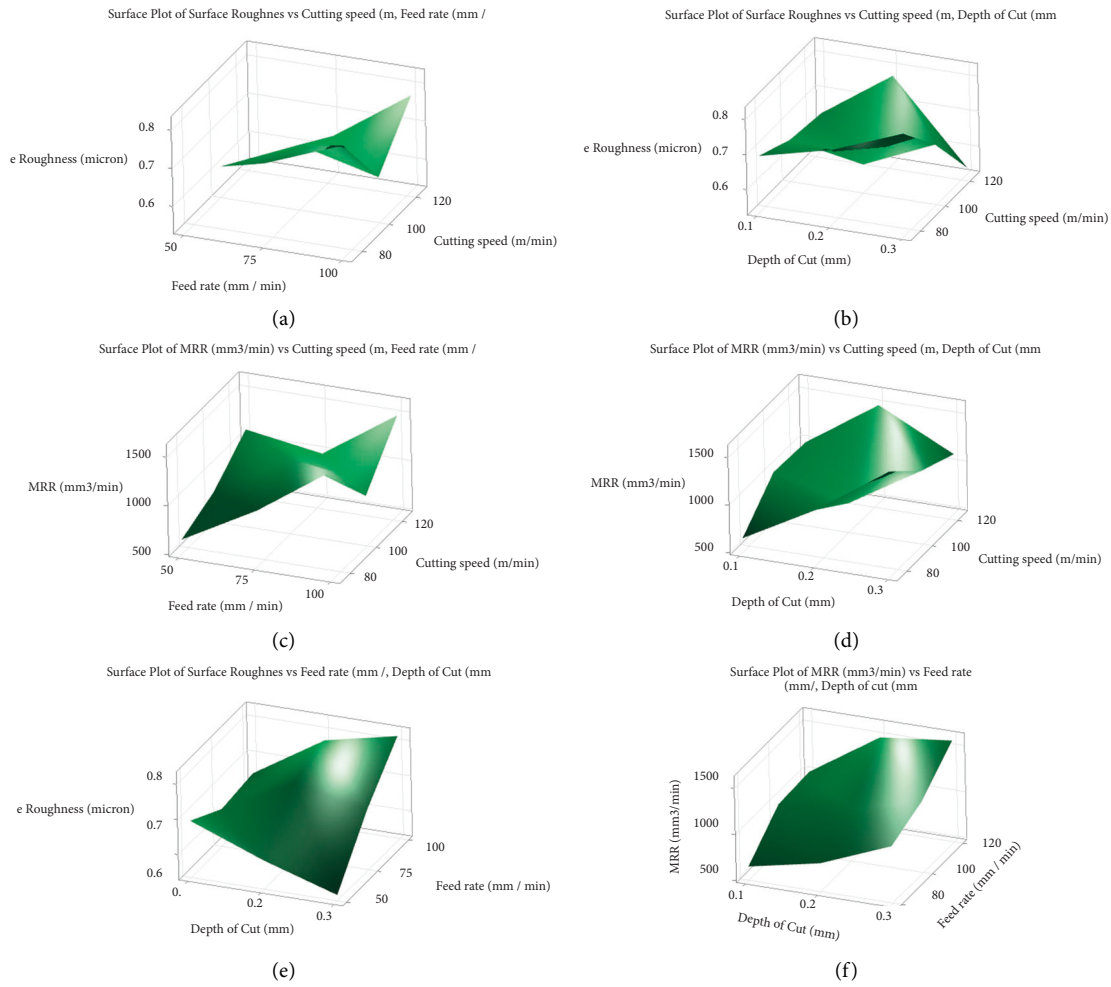

Figure 6: Surface plot of MRR at depth of cut with the variable levels of 0.1, 0.2, and 0.3 mm, respectively. (a) Surface roughness versus feed rate. (b) Surface roughness versus depth of cut. (c) MRR versus cutting speed. (d) MRR versus depth of cut. (e) Surface roughness versus feed rate. (f) MRR versus depth of cut.

Table 8: ANOVA results for SR and MRR responses.

Source (SR)	DF	Seq SS	Contribution	Adj SS	Adj MS	F value	P value
Cutting speed	2	0.019144	32.62%	0.019144	0.009572	2.12	0.032
Feed rate	2	0.026614	45.34%	0.026614	0.013307	2.95	0.025
Depth of cut	2	0.003908	6.66%	0.003908	0.001954	0.43	0.069
Error	2	0.009028	15.38%	0.009028	0.004514		
Total	8	0.058694	100.00%				
Source (MRR)	DF	Seq SS	Contribution	Adj SS	Adj MS	F value	P value
Cutting speed	2	46101	6.11%	46101	23050	4.37	0.086
Feed rate	2	399402	52.94%	399402	199701	37.82	0.026
Depth of cut	2	298451	39.56%	298451	149225	28.26	0.034
Error	2	10561	1.40%	10561	5280		
Total	8	754514	100.00%				

rate, is 0.98. Regression analysis for the material removal rate and best fit equation for the material removal rate will be shown in

$$\text{MRR} = -274 + 0.0502\,\text{Spindle speed} + 10.32\,\text{Feed rate} + 2227\text{cut}. \quad (4)$$

Similarly, the R-square value relating to the output response, such as surface roughness, is 0.96. Regression analysis for the surface roughness and best fit equation for the surface roughness is shown in

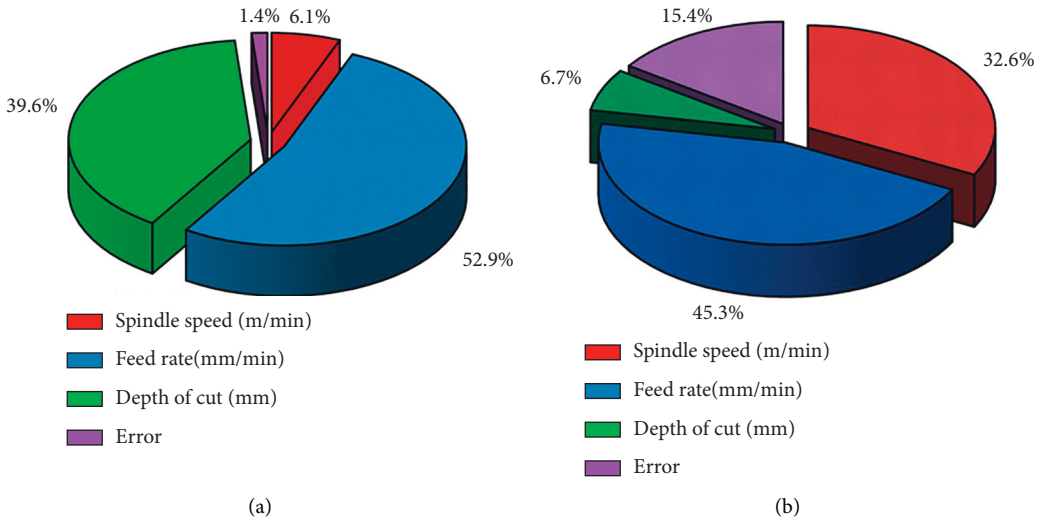

Figure 7: Percentage contribution chart, (a) material removal rate, and (b) surface roughness.

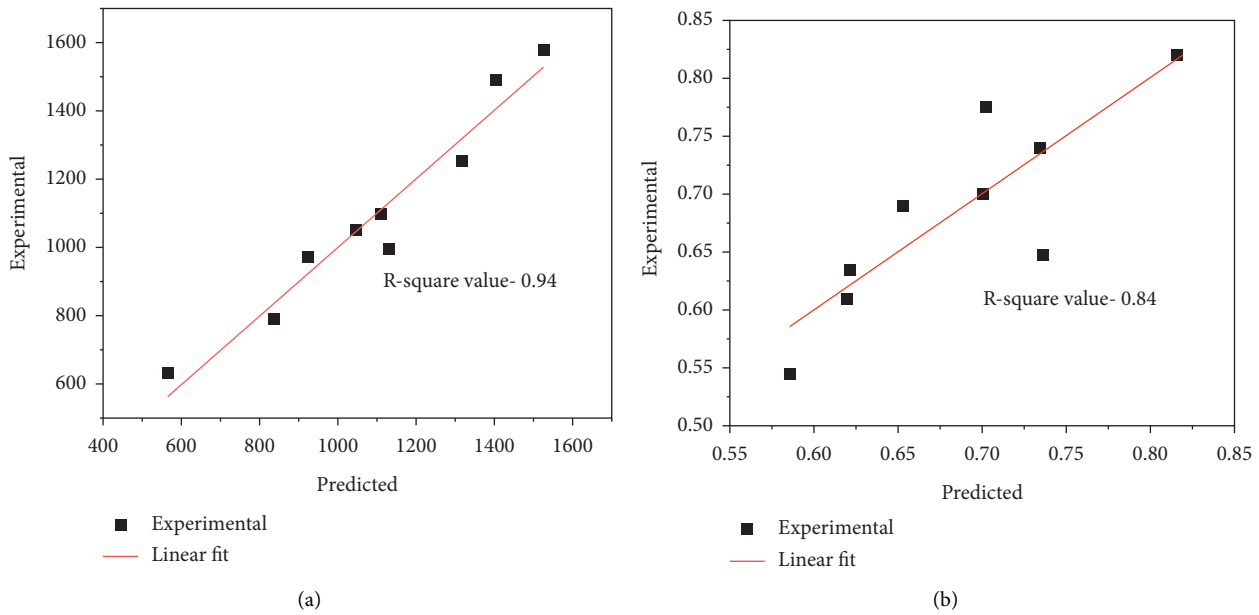

Figure 8: *R*-square fit: (a) material removal rate (mm^3/min) and (b) surface roughness (μm).

$$\text{Ra} = 0.603 - 0.000049\,\text{Cutting speed} + 0.002653\text{Feed rate} + 0.153\,\text{Depth of cut}. \quad (5)$$

3.5. Confirmation Experiment for the Material Removal Rate and Surface Roughness. The confirmation experiment for the optimal combination of the end milling experiment for the DMLS Inconel 718 alloy was presented using the regression equation. Table 9 shows the optimal combination of the milling experiments' surface roughness and material removal rate. The optimal combination for the AM Inconel 718 alloy milling experiment was found using the Taguchi analysis. The predicted and experimental material removal rates were 665.1 and 641 (mm^3/min) from the experimental results. The error percentage was 3.82%, which is an acceptable limit. Likewise, for the response surface roughness response analysis, the predicted and experimental surface roughness values were 0.7182 and 0.7021 μm. And the error percentage was 2.30%. Both the output responses are within the acceptable range of error value. Sabarinathan et al. also observed a similar error percentage in the recovery of the sol-gel alumina abrasive grain process [29].

3.6. Estimation of 3D Surface Roughness for the Optimized Condition. Figure 9 shows the 3D surface roughness plot of the optimized machining condition. The results show that

Table 9: Confirmation experiments for the optimum conditions of material removal rate and surface roughness.

Output responses	Optimal combination	Predicted value	Experimental value	Percentage error
Material removal rate (mm^3/min)	Cutting speed, 125 Feed rate, 100 Depth of cut, 0.3	665.5	641	3.82
Surface roughness (μm)	Cutting speed, 125 Feed rate, 50 Depth of cut, 0.1	0.7182	0.7021	2.30

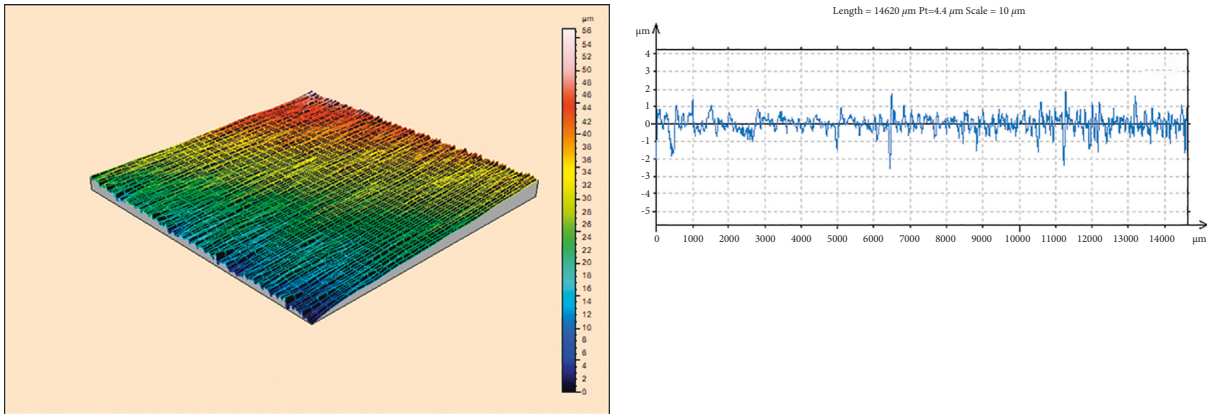

(a) (b)

Figure 9: 3D surface roughness plot for the optimized machining condition.

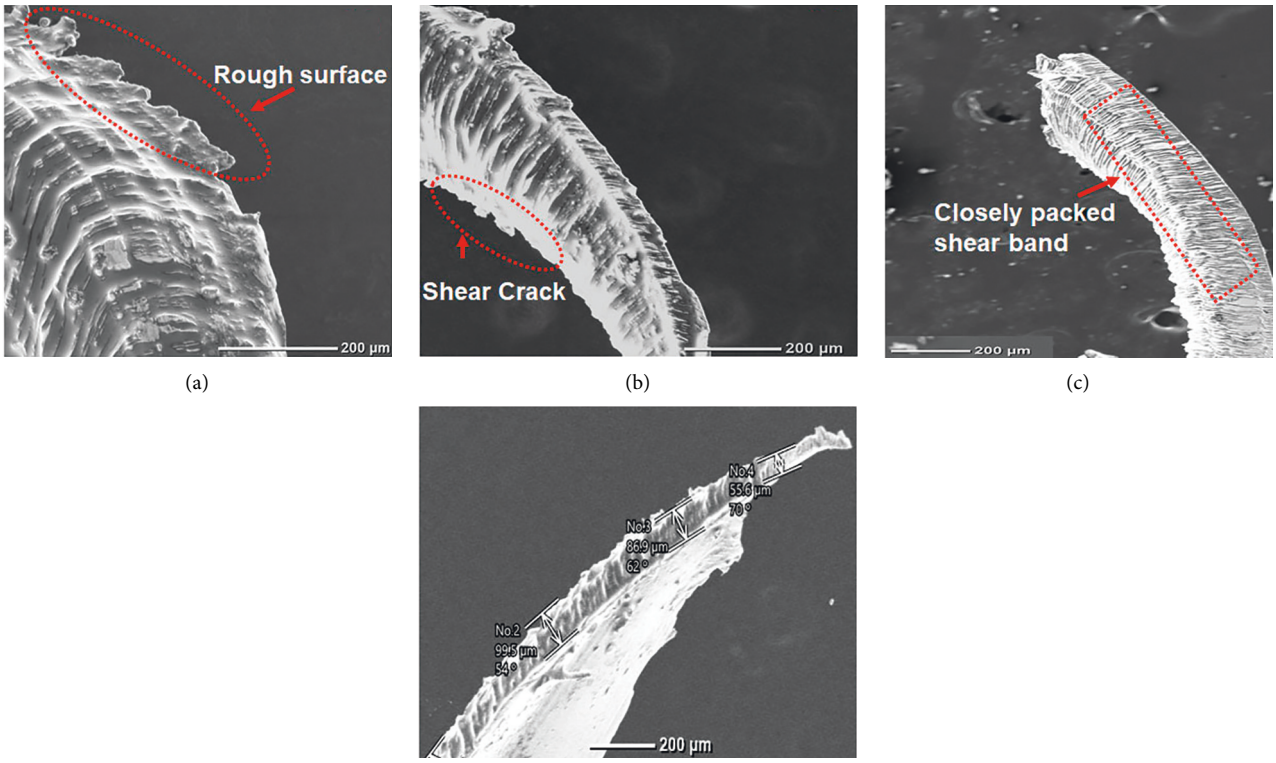

(a) (b) (c)

(d)

Figure 10: Chip morphology of the machined DMLS component.

the lowest surface roughness value of 0.7021 μm was observed under the respective condition. Likewise, the Arial surface roughness parameters, such as arithmetic mean deviation of the surface (Sa) and Kurtosis of the Topography Height Distribution (Sku), were found on the machined DMLS Inconel 718 alloy by using a 3D surface profilometer. The results show that the average mean deviation (Sa) was 7.87 μm, and Kurtosis of the Topography Height Distribution (Sku) was 2.52 μm obtained for the optimized machining condition.

3.7. Examination of Chip Morphology of DMLS Inconel 718 Plate. Figure 10 shows the chip morphology of the machined AM component with two different cutting speeds. Figures 10(a) and 10(b) show the machining condition for 75 m/min cutting speed. The results show that there is an observance of tubular helical shape profiles observed on the surfaces of the chip. Figure 10(c) shows the presence of shear crack; this is the main finding which is the reason for poor surface finish and increases the surface roughness of the machined surface. This may result in craters and valleys in the machined surfaces. Anand and Mathew reported a similar trend of outcomes on the chip morphology on the Inconel 718 alloy [30]. Figure 10(d) shows a higher cutting speed of 125 m/min and the chip morphology. The results show that there is a closely packed shear band present on the chip surface. This phenomenon occurred due to thermal softening and smoothening of the contact zone. It results in a smoother surface finish occurring on the machined surface. Similarly, for higher cutting speed, feed, and depth of cut, a maximum chip thickness of 99.5 μm was observed on the DMLS Inconel 718 alloy.

4. Conclusions

The paper mainly emphasises the process optimization of the end milling study of the fabricated Inconel 718 plate via the DMLS method. The optimization was carried out for the end milling study using the Taguchi technique. Summarised inferences are listed as follows:

(i) The optimized combination for the higher material removal rate of the end milling process for the DMLS Inconel 718 plate was analysed using Taguchi analysis. The optimal combination for obtaining high material removal rate of Inconel alloy is cutting speed of 125 m/min, feed rate of 100 mm/min, and depth of cut of 0.3 mm.

(ii) The identified optimal combination for the minimum surface roughness value is the lowest feed rate of 50 mm/min, the highest cutting speed of 125 m/min, and the lowest depth of cut of 0.1 mm.

(iii) The influencing parameter sequence and the highest contribution for the material removal rate are ordered as follows: feed rate > cutting speed > depth of cut. Each control factor contribution percentage obtaining the highest material removal rate is feed rate, depth of cut, and cutting speed. It has influenced the material removal rate by 52.93%, 39.55%, and 6.10%, respectively.

(iv) The sequence of influencing parameters for the surface roughness response is feed rate > depth of cut > cutting speed, and the percentage contribution was feed rate of 45.34%, followed by cutting speed of 32.61% and depth of cut of 6.66%.

(v) The regression analysis shows that the material removal rate and surface roughness error percentage are 3.82 and 2.30%.

(vi) SEM observation revealed that, for lower cutting speed, the chips have surface irregularities and shear crack, decreasing the machined surfaces' surface smoothness.

(vii) The regression analysis and developed mathematical model can correlate the experimental results for the end milling experiment of DMLS Inconel 718 alloy.

Data Availability

The data used to support the findings of this study are included within the article and further data or information can be obtained from the corresponding author upon request.

Disclosure

This study was performed as a part of the Employment of Wollo University, Kombolcha Institute of Technology, Ethiopia.

Conflicts of Interest

The authors declare that there are no conflicts of interest regarding the publication of this paper.

Acknowledgments

The authors acknowledge the Indira Gandhi Centre for Atomic Research, Kalpakkam, Chennai Institute of Technology, and Saveetha School of Engineering, SIMATS, Chennai, for the technical assistance. The authors appreciate the support from Wollo University, Kombolcha Institute of Technology, Ethiopia.

References

[1] K. R. Ryan, M. P. Down, and C. E. Banks, "Future of additive manufacturing: overview of 4D and 3D printed smart and advanced materials and their applications," *Chemical Engineering Journal*, vol. 403, Article ID 126162, 2021.

[2] H. Shirvani, H. Mebrahtu, and J. Butt, "Numerical and experimental analysis of product development by composite metal foil manufacturing," *International Journal of Rapid Manufacturing*, vol. 7, no. 1, pp. 59–82, 2018.

[3] K. S. Boparai, R. Singh, F. Fabbrocino, and F. Fraternali, "Thermal characterization of recycled polymer for additive manufacturing applications," *Composites Part B: Engineering*, vol. 106, pp. 42–47, 2016.

[4] P. Sureshkumar, T. Jagadeesha, L. Natrayan, M. Ravichandran, D. Veeman, and S. M. Muthu, "Electrochemical corrosion and tribological behaviour of AA6063/Si3N4/Cu (NO3) 2 composite processed using single-pass ECAPA route with 120 die angle," *Journal of Materials Research and Technology*, vol. 16, pp. 715–733, 2022.

[5] G. Sur and Ö. Erkan, "Surface quality optimization of CFRP plates drilled with standard and step drill bits using TAGUCHI, TOPSIS and AHP method," *Engineering Computations*, vol. 38, no. 5, pp. 2163–2187, 2021.

[6] G. Sur and Ö. Erkan, "Cutting tool geometry in the drilling of cfrp composite plates and taguchi optimisation of the cutting parameters affecting delamination," *Sigma Journal of Engineering and Natural Sciences*, vol. 36, no. 3, pp. 619–628, 2018.

[7] E. Altas, O. Erkan, D. Ozkan, and H. Gokkaya, "Optimization of cutting conditions, parameters, and cryogenic heat treatment for surface roughness in milling of NiTi shape memory alloy," *Journal of Materials Engineering and Performance*, vol. 31, 2022.

[8] Ö. Erkan, G. Sur, and E. Nas, "Investigation of surface morphology of drilled CFRP plates and optimization of cutting parameters," *Surface Review and Letters*, vol. 27, no. 09, Article ID 1950209, 2020.

[9] A. Rajesh Kannan, S. Mohan Kumar, N. Pravin Kumar, N. Siva Shanmugam, A. S. Vishnu, and Y. Palguna, "Process-microstructural features for tailoring fatigue strength of wire arc additive manufactured functionally graded material of SS904L and Hastelloy C-276," *Materials Letters*, vol. 274, Article ID 127968, 2020.

[10] B. Anush Raj, J. Winowlin Jappes, M. Adam Khan, V. Dillibabu, and N. C. Brintha, "Direct metal laser sintered (DMLS) process to develop Inconel 718 alloy for turbine engine components," *Optik*, vol. 202, Article ID 163735, 2020.

[11] G. P. Dinda, A. K. Dasgupta, and J. Mazumder, "Laser aided direct metal deposition of Inconel 625 superalloy: microstructural evolution and thermal stability," *Materials Science and Engineering: A*, vol. 509, no. 1-2, pp. 98–104, 2009.

[12] I. A. Choudhury and M. A. El-Baradie, "Machinability of nickel-base super alloys: a general review," *Journal of Materials Processing Technology*, vol. 77, no. 1-3, pp. 278–284, 1998.

[13] M. Karthick, P. Anand, M. Meikandan, S. Sekar, L. Natrayan, and K. Bobe, "Optimization of plasma arc cutting parameters on machining of Inconel 718 superalloy," *Journal of Nanomaterials*, vol. 2022, Article ID 7181075, 13 pages, 2022.

[14] A. Shokrani, V. Dhokia, and S. T. Newman, "Environmentally conscious machining of difficult-to-machine materials with regard to cutting fluids," *International Journal of Machine Tools and Manufacture*, vol. 57, pp. 83–101, 2012.

[15] S. Zahoor, F. Ameen, W. Abdul-Kader, and J. Stagner, "Environmentally conscious machining of Inconel 718: surface roughness, tool wear, and material removal rate assessment," *International Journal of Advanced Manufacturing Technology*, vol. 106, no. 1-2, pp. 303–313, 2020.

[16] T. Thepsonthi and T. Özel, "Multi-objective process optimization for micro-end milling of Ti-6Al-4V titanium alloy," *International Journal of Advanced Manufacturing Technology*, vol. 63, no. 9-12, pp. 903–914, 2012.

[17] J. W. Ma, F. J. Wang, Z. Y. Jia, Q. Xu, and Y. Y. Yang, "Study of machining parameter optimization in high speed milling of Inconel 718 curved surface based on cutting force," *International Journal of Advanced Manufacturing Technology*, vol. 75, no. 1-4, pp. 269–277, 2014.

[18] R. Anburaj and M. Pradeep Kumar, "Experimental studies on cryogenic CO2 face milling of Inconel 625 superalloy," *Materials and Manufacturing Processes*, vol. 36, no. 7, pp. 814–826, 2021.

[19] F. Jiang, J. Li, L. Yan, J. Sun, and S. Zhang, "Optimizing end-milling parameters for surface roughness under different cooling/lubrication conditions," *International Journal of Advanced Manufacturing Technology*, vol. 51, no. 9-12, pp. 841–851, 2010.

[20] B. Sarkar, M. M. Reddy, and S. Debnath, "Effect of machining parameters on surface finish of Inconel 718 in end milling," *MATEC Web of Conferences*, vol. 95, Article ID 02009, 2017.

[21] S. K. Shihab, J. Gattmah, and H. M. Kadhim, "Experimental investigation of surface integrity and multi-objective optimization of end milling for hybrid Al7075 matrix composites," *Silicon*, vol. 13, no. 5, pp. 1403–1419, 2021.

[22] D. Chalawadi, S. P. K. Babu, and V. Dhinakaran, "Experimental investigation of TIG welded additive manufactured inco-718 sheets," *Materials Research*, vol. 23, no. 2, 2020.

[23] R. K. Roy, *Design of experiments using the Taguchi approach: 16 steps to product and process improvement*, John Wiley & Sons, Hoboken, NJ, USA, 2001.

[24] Y. Kaynak, A. Gharibi, U. Yılmaz, U. Köklü, and K. Aslantaş, "A comparison of flood cooling, minimum quantity lubrication and high pressure coolant on machining and surface integrity of titanium Ti-5553 alloy," *Journal of Manufacturing Processes*, vol. 34, pp. 503–512, 2018.

[25] S. Zahoor, N. A. Mufti, M. Q. Saleem, M. P. Mughal, and M. A. M. Qureshi, "Effect of machine tool's spindle forced vibrations on surface roughness, dimensional accuracy, and tool wear in vertical milling of AISI P20," *International Journal of Advanced Manufacturing Technology*, vol. 89, no. 9-12, pp. 3671–3679, 2017.

[26] X. Lu, F. Wang, L. Xue, Y. Feng, and S. Y. Liang, "Investigation of Material Removal Rate and Surface Roughness Using Multi-Objective Optimization for Micro-milling of Inconel 718," *Industrial lubrication and Tribology*, vol. 71, no. 6, pp. 787–794, 2019.

[27] S. Mohan Kumar, S. Sankarapandian, and N. Siva Shanmugam, "Investigations on mechanical properties and microstructural examination of activated TIG-welded nuclear grade stainless steel," *Journal of the Brazilian Society of Mechanical Sciences and Engineering*, vol. 42, no. 6, pp. 292–321, 2020.

[28] P. Sabarinathan, V. E. Annamalai, R. Balakrishnan, and A. C. Kuriakose, "Process optimization for recovery of fiber backing from coated abrasive disks," *Chemical Engineering Communications*, vol. 208, no. 6, pp. 893–902, 2021.

[29] P. Sabarinathan and V. E. Annamalai, "Removal of aluminosilicate bond and process optimization on recovery of sol gel alumina abrasive grain from abrasive industry waste," *Silicon*, vol. 13, no. 2, pp. 495–505, 2021.

[30] K. N. Anand and J. Mathew, "Evaluation of size effect and improvement in surface characteristics using sunflower oil-based MQL for sustainable micro-endmilling of Inconel 718," *Journal of the Brazilian Society of Mechanical Sciences and Engineering*, vol. 42, no. 4, pp. 156–213, 2020.